Development 125, 4729-4738 (1998)
Printed in Great Britain © The Company of Biologists Limited 1998
DEV5242

Functional analysis of Wingless reveals a link between intercellular ligand transport and dorsal-cell-specific signaling

Herman A. Dierick and Amy Bejsovec*

Department of Biochemistry, Molecular Biology and Cell Biology, Northwestern University, 2153 Sheridan Road, Evanston, IL 60208-3500, USA
*Author for correspondence (e-mail: bejsovec@nwu.edu)

Accepted 17 September; published on WWW 9 November 1998

SUMMARY

The *Drosophila* segment polarity gene *wingless* (*wg*) is essential for cell fate decisions in the developing embryonic epidermis. Wg protein is produced in one row of cells near the posterior of every segment and is secreted and distributed throughout the segment to generate wild-type pattern elements. Ventrally, epidermal cells secrete a diverse array of anterior denticle types and a posterior expanse of naked cuticle; dorsally, a stereotyped pattern of fine hairs is secreted. We describe three new *wg* alleles that promote naked cuticle cell fate but show reduced denticle diversity and dorsal patterning. These mutations cause single amino acid substitutions in a cluster of residues that are highly conserved throughout the Wnt family. By manipulating expression of transgenic proteins, we demonstrate that all three mutant molecules retain the intrinsic capacity to signal ventrally but fail to be distributed across the segment. Thus, movement of Wg protein through the epidermal epithelium is essential for proper ventral denticle specification and this planar movement is distinct from the apical-basal transcytosis previously described in polarized epithelia. Furthermore, ectopic overexpression of the mutant proteins fails to rescue dorsal pattern elements. Thus we have identified a region of Wingless that is required for both the transcytotic process and signal transduction in dorsal cell populations, revealing an unexpected link between these two aspects of Wg function.

Key words: Wingless, Transcytosis, Pattern formation, Signal transduction, *Drosophila*

INTRODUCTION

Wingless (Wg) is the *Drosophila* ortholog of vertebrate Wnt-1 (Rijsewijk et al., 1987) and belongs to the Wnt family of secreted growth factors (reviewed in Nusse and Varmus, 1992; Dierick and Bejsovec, 1998). Wnts are larger than other known growth factors and do not appear to be cleaved; for example, Wg is 468 amino acids long, compared with epidermal growth factor, which is 53 amino acids long. Furthermore, Wnts associate tightly with membrane and extracellular matrix (Bradley and Brown, 1990; Papkoff and Schryver, 1990) and have not yet been purified in soluble active form (Nusse et al., 1997). These properties suggest that Wnts may require cellular handling beyond the simple secretion and diffusion typical of other growth factors.

Members of the Wnt family control cell fate decisions during the development of organisms as diverse as nematodes and humans. In *Drosophila*, Wg specifies cell fate in a wide variety of tissues at different developmental stages. In many cases, *wg* is expressed in a defined domain within the tissue but affects cellular decisions over a broader domain, suggesting that the secreted gene product acts at a distance either directly or through a relay mechanism. In imaginal discs, a membrane-tethered form of Wg promotes molecular responses over a much shorter range of cells than is observed for the wild-type, untethered molecule, consistent with a direct long-range mechanism of Wg action (Zecca et al., 1996). Likewise, Wnt molecules in cell culture appear to promote morphological changes over many cell diameters from the *Wnt*-expressing cell population (Jue et al., 1992; Parkin et al., 1993). This raises the question of how a molecule that associates tightly with membranes and extracellular matrix is able to promote direct response in cells at a distance from the source of gene product.

Active cellular processes are required for the broad distribution of Wg protein and its consequent signaling activity. The *shibire (shi)* mutation (van der Bliek and Meyerowitz, 1991) was used to inhibit endocytosis during embryogenesis, and it concomitantly restricts Wg protein distribution and Wg signaling function (Bejsovec and Wieschaus, 1995). In wild-type embryos, *wg* is expressed in a single row of cells in each segment (Baker, 1987), but Wg protein is detected in a broad punctate distribution over many cell diameters on either side of the *wg*-expressing cells (van den Heuvel et al., 1989; Gonzalez et al., 1991). In *shi* mutant embryos, Wg protein accumulates around the *wg*-expressing cells. This restricted distribution of Wg protein correlates with restricted signaling activity, as measured by stabilization of Armadillo (Arm) protein (Riggleman et al., 1990; Peifer et al., 1991). Stable Arm provides a transactivation domain when complexed with the transcription factor, dTCF,

and thereby drives expression of Wg target genes, such as *engrailed* (Brunner et al., 1997; Riese et al., 1997; van de Wetering et al., 1997). In wild-type embryos, Wg-mediated Arm stabilization extends over 3 to 4 cell diameters on either side of the *wg*-expressing row of cells in each segment. In *shi* mutants, Arm stripes are narrower and extend only one cell diameter on either side of the *wg* domain (Bejsovec and Wieschaus, 1995). These observations suggest that Wg protein is actively moved between and across cells in a process that requires endocytic components. This form of transcytotic movement is directed laterally in the plane of the polarized epidermal epithelium and therefore differs from previously characterized apical-basal transcytosis across polarized epithelia (reviewed in Rodman et al., 1990; Mostov, 1994).

It is not clear whether all aspects of this phenomenon are regulated by the general endocytic machinery or if molecules specific to Wg transport are required. As a first step toward defining the Wg transport pathway, we have identified and characterized mutations within *wg* that disrupt this process. Remarkably, each of three independent missense changes also disrupts Wg signal transduction in dorsal, but not ventral, epidermal cell populations. Thus we have discovered an unprecedented link between Wg transport and dorsal signaling, which may suggest the existence of an extracellular component common to both processes, and which may help to explain puzzling previous observations about the timing of Wg-mediated pattern specification.

MATERIALS AND METHODS

Fly stocks

wg^{PE6}, wg^{NE1} and wg^{NE2} were induced by ethyl methanesulfonate mutagenesis and isolated by failure to complement the adult viable wg^{1} allele (Sharma and Chopra, 1976). *Df(2)DE* (Tiong and Nash, 1990) is a small deficiency that removes part of the *wg* promoter but leaves intact the coding region (A. B., unpublished) and was a gift from S. Tiong. *Df(2)DE* homozygotes show defects in cuticle deposition, and so this deficiency was placed in *trans* with wg^{CX4} to assess cuticle pattern. wg^{CX4} produces no detectable RNA (Baker, 1987). wg^{IL114} is a temperature-sensitive allele that produces non-functional gene product at 25°C (Bejsovec and Martinez-Arias, 1991). All *wg* alleles are maintained over the *CyO* balancer.

RNA extraction, RT-PCR and sequence analysis

Embryos from heterozygous parents were collected on apple juice agar plates for 8 hours, dechorionated with bleach, washed in water and frozen in liquid nitrogen. Total RNA was extracted using Trizol Reagent (Gibco-BRL). Reverse transcription-polymerase chain reaction (RT-PCR) and PCR were performed using standard protocols (Promega, Perkin Elmer). Primers spanning positions 369 (5′CAGTGTGAGAGTGTGTGTGCC3′) and 1990 (5′GCATGGT-ACACTTTAGGGGCGG3′), respectively, in the *wg* cDNA (Rijsewijk et al., 1987) amplify a 1622 bp fragment. Purified PCR product was subjected to single-stranded PCR using an internal primer; both strands were sequenced using primers that span the entire cDNA. Two of the mutations alter restriction endonuclease sites and were confirmed by restriction digestion of PCR products. A 475 bp fragment between positions 571 and 1045 in the *wg* cDNA has two *Hha*I sites, one of which is eliminated by the wg^{PE6} mutation. A 522 bp fragment between positions 1087 and 1608 contains an *Rsa*I site, which is eliminated by the wg^{NE2} mutation.

Transgene construction and analysis

The wg^{PE6}, wg^{NE1} and wg^{NE2} mutations were engineered into wild-type *wg* cDNA using the Unique Site Elimination (USE) mutagenesis kit (Pharmacia). Plasmids were sequenced completely to verify the mutation and to screen for undesirable errors before subcloning into the pUAST expression vector (Brand and Perrimon, 1993). pUAST was modified to include a polyadenylation site flanked by two FLP recombinase target sites between promoter and coding sequence. This prevents transient expression in injected embryos, enhancing recovery of germline transformants, and can be removed from transgenic animals by introducing FLP recombinase (Buenzow and Holmgren, 1995). Plasmids were purified using Qiagen columns and injected into *y w*; *Δ2-3 Sb*/*TM3 e* embryos for germline transformation (Spradling, 1986).

UAS-wg transgenes were activated using *prd-GAL4*, which drives expression in the 5-cell-wide *paired* domain spanning the *wg*- and *engrailed(en)*-expressing rows of cells in odd-numbered segments (Yoffe et al., 1995), and *E22C-GAL4*, a constitutive ubiquitous driver line available from the Bloomington Stock Center. All transgenes were analyzed in the wg^{CX4} mutant background to assess rescue of the null mutant phenotype. Several germline transformants were recovered for each *UAS-wg* transgene. Each was tested for expression level with the *wg-GAL4* driver (gift of J. Pradel); those lines that reproduced the phenotype of the original mutant stock were selected for analysis.

Cuticle preparation and immunohistochemistry

For cuticle preparation, embryos were allowed to age at either 18°C or 25°C, dechorionated and mounted in Hoyer's medium/lactic acid as described in Wieschaus and Nüsslein-Volhard (1986). For antibody staining, embryos were dechorionated, devitellinized in methanol/heptane and fixed with 4% formaldehyde in PEM buffer (0.1 M Pipes, 1 mM EDTA, 2 mM $MgSO_4$, pH 6.9). Preincubation with 10% bovine serum albumin (BSA) was used to block nonspecific binding and subsequent washes were performed with 1% BSA in phosphate-buffered saline supplemented with 0.1% Tween 20. Anti-Wg antibody was used at 1:1,000 (gift from S. Cumberledge), anti-En was used at 1:50 (gift from M. Peifer) and anti-Arm was used at 1:400 (gift from E. Wieschaus). Biotinylated secondary antibody (Zymed) and avidin-biotin-complex (ABC kit from Vector Labs) were used for diaminobenzidine staining, and embryos were dehydrated, cleared in xylene and mounted in DPX mounting medium (Aldrich). Rhodamine secondary antibody (Boehringer Mannheim) was used for fluorescent labeling and embryos were mounted in Aquapolymount (Polysciences) and viewed with a laser scanning confocal microscope (Biorad MRC 600). *wg* RNA in situ hybridization was performed according to Tautz and Pfeifle (1989).

Embryos were staged according to Campos-Ortega and Hartenstein (1985). Homozygous *wg* mutant embryos were chosen for photography based on distinctive morphological defects apparent in later stages of development. These defects include enlarged and/or deformed tracheal pits and abnormal segmental furrows.

RESULTS

wg^{PE6}, wg^{NE1} and wg^{NE2} mutant embryos show restricted Wg response

In late-stage *Drosophila* embryos, epidermal cells secrete a segmentally repeating pattern of cuticular structures: six rows of uniquely shaped, hook-like denticles interspersed with naked cuticle on the ventral surface and fine hairs on the dorsal surface (Lohs-Schardin et al., 1979; Campos-Ortega and Hartenstein, 1985; Wieschaus and Nüsslein-Volhard, 1986). Wg signaling during earlier stages is required for correct specification of these cuticular pattern elements (reviewed in Bejsovec and Peifer, 1996). *wg* null mutants (Fig. 1A) secrete no ventral naked cuticle and instead produce denticles consisting primarily of a single morphology; this denticle type resembles the large refractile denticles found in the fifth row of the wild-type

denticle belt (Bejsovec and Wieschaus, 1993). *wg* mutant denticles are arranged in a segmentally repeating pattern of reversed polarity whereas, on the dorsal surface, no segmental pattern is observed and all cells secrete a single type of hair (Nüsslein-Volhard and Wieschaus, 1980; Baker, 1988; Bejsovec and Martinez-Arias, 1991). Ectopic Wg restores belts of diverse denticle types when provided at low level in a *wg* null mutant (Sampedro et al., 1993; Hays et al., 1997), and produces uniform naked cuticle when provided at high level (Hays et al., 1997). Thus the ventral denticle-secreting cells, which lie at the greatest distance from the *wg*-expressing row of cells, may serve as indicators of long-range Wg protein transport, while the naked cuticle region, which is roughly centered over the *wg*-expressing row of cells (Dougan and DiNardo, 1992), serves as a marker for short-range, high-level Wg activity. Alternatively, it is possible that denticle diversity is generated indirectly by a short-range relay mechanism triggered by Wg. However, experiments with a temperature-sensitive *wg* allele have shown that denticle diversity is specified by Wg activity at early stages of development (Bejsovec and Martinez-Arias, 1991), making a multiple step process less likely.

Three novel alleles of *wg* secrete some ventral naked cuticle and alter denticle diversity to different degrees, but dorsally they show little or no Wg-mediated patterning. Two alleles, wg^{PE6} and wg^{NE1}, are temperature sensitive. At 25°C, mutant embryos display more segmentation than a *wg* loss-of-function mutant and produce denticle morphologies other than row-5 type, but only at a low frequency (Figs 1B,C, 2). The wg^{NE2} allele produces the same pattern at both 18°C and 25°C: mutant embryos secrete patches of naked cuticle and belts containing predominantly row-5-type denticles, with a low frequency of other denticle morphologies (Figs 1D, 2). The wg^{NE1} allele at 18°C resembles wg^{NE2} (Fig. 1E), whereas the wg^{PE6} mutant at 18°C shows dramatic improvement, with almost wild-type pattern on the ventral surface, but limited patterning of the dorsal surface (Figs 1F,G, 2).

The restricted cuticular patterning of the mutant embryos is mirrored by molecular markers of Wg activity. All three alleles produce protein that accumulates at high level in the *wg*-expressing cells and shows little accumulation in neighboring cells (Fig. 3A-D). Arm protein, which normally accumulates in broad stripes centered over the *wg*-expressing row of cells (Fig. 3E), shows no accumulation in wg^{NE2} mutant embryos at either 18°C or at 25°C (Fig. 3F), even though the ventral cuticle pattern shows evidence of Wg activity. This suggests that amounts of stable Arm below the level of detection are able to mediate Wg specification of cuticular pattern elements. Likewise, wg^{NE1} and wg^{PE6} mutant embryos cultured at 25°C show no detectable stripes of Arm accumulation but, in embryos cultured at 18°C, faint and very narrow stripes of higher Arm staining can be observed (Fig. 3G,H). These Arm stripes are similar in width to those observed when endocytosis is blocked by *shi* mutation (Bejsovec and Wieschaus, 1995). Thus in wg^{NE1} and wg^{PE6} mutants, as in *shi* mutants, the range of cells over which Wg can signal is reduced.

Expression of the Wg-responsive gene, *engrailed (en)* also provides an assay for Wg signal transduction in neighboring, non-*wg*-expressing cells. Wg activity is required for the maintenance of *en* expression in the adjacent posterior two rows of cells; in the absence of *wg* gene function, epidermal *en* expression is initiated normally but decays during stages 9 and 10 (DiNardo et al., 1988; Martinez Arias et al., 1988). In wg^{PE6} and wg^{NE1}

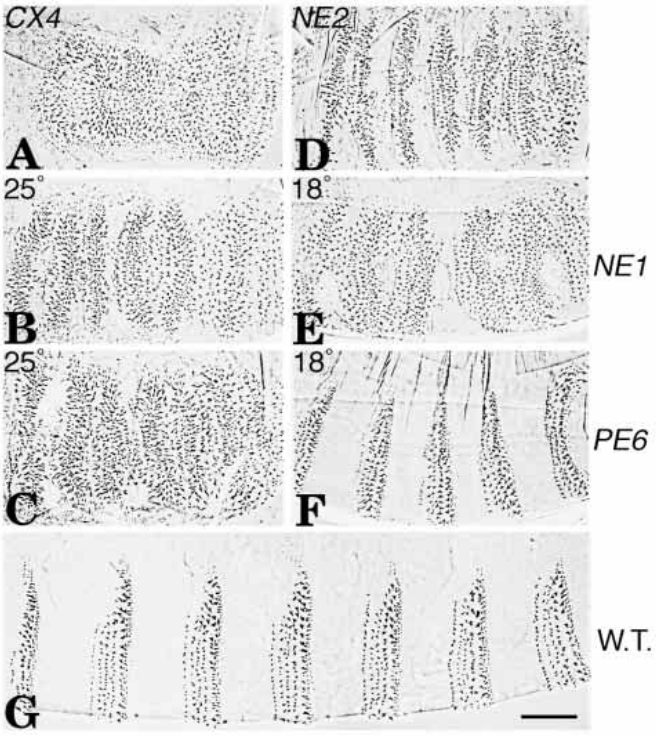

Fig. 1. Allelic series of partial function *wg* mutations. (A) Cuticle pattern produced by wg^{CX4} null mutants. In this and all subsequent photographs, anterior of the embryo is to the left. (B) wg^{NE1} mutant embryos at 25°C, and (C) wg^{PE6} mutant embryos at 25°C show more segmentation. (D) wg^{NE2} mutant embryos at both 18° and 25°C (shown) and (E) wg^{NE1} mutant embryos at 18°C secrete more denticle types and some naked cuticle. (F) wg^{PE6} mutants at 18°C produce an almost wild-type ventral pattern. Dorsal patterning is disrupted, causing all embryos to appear curved compared to wild-type, (G). Scale bar is 100 μm.

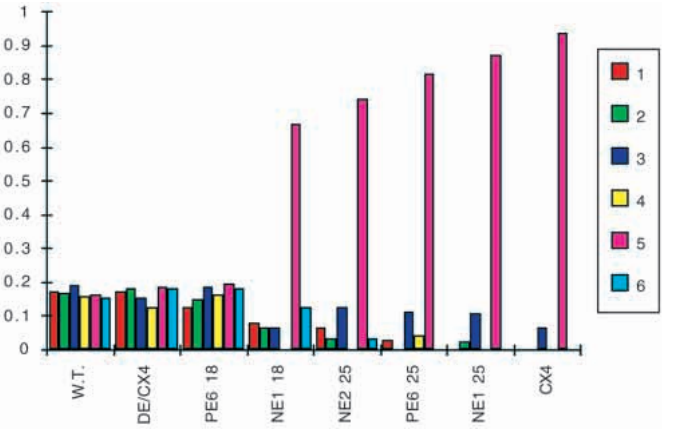

Fig. 2. Quantification of denticle diversity. Bars represent each of six distinct denticle types expressed as a percentage of total denticles scored. A fixed field spanning the ventral region of the fourth abdominal segment was examined and each denticle within the field was assigned to the denticle type category that it most closely resembled. Twelve embryos per genotype were analyzed, with a total of over 400 denticles per genotype scored. Criteria for scoring denticle types are described in Bejsovec and Wieschaus (1993).

mutant embryos at 25°C, as in *wg* null mutants, *en* is expressed normally at early stages but, by stage 11, no epidermal *en* expression is reproducibly detected (not shown). In wg^{NE2} mutants (Fig. 3J), and in wg^{NE1} and wg^{PE6} at 18°C (Fig. 3K,L) *en* expression decays in a defined pattern: stabilized *en* expression can be seen only in the most ventral cells of the *en* stripe, with little or no stabilization in dorsal and dorsolateral cells. The severity of phenotype in the allelic series correlates with the number of cells that stably maintain *en* expression: wg^{NE2} mutant embryos show single, isolated *en*-expressing cells, whereas wg^{PE6} embryos at 18°C show an almost intact 1- to 2-cell-wide stripe over the ventral region. Stabilization of *en* expression in neighboring cells indicates that the mutant molecules can move through the secretory pathway to the cell surface.

The autocrine function of Wg is not disrupted significantly by these mutations. Wg activity is required for *wg* autoregulation; in the absence of *wg* gene function, *wg* expression decays by stage 10 (Bejsovec and Martinez-Arias, 1991; Ingham and Hidalgo, 1993). All three partial function alleles at either temperature express *wg* RNA beyond stage 11 (Fig. 4C,D). In contrast, the paracrine Wg response, as measured by stabilization of later *en* expression, is eliminated in dorsal cell populations and is limited in ventral populations to those cells that directly contact the *wg*-expressing cells. Thus these mutational changes appear to perturb those activities of Wg that require transit between or through cells.

wg^{PE6}, wg^{NE1} and wg^{NE2} do not simply reduce Wg function

Limited paracrine function of the mutant proteins could result from lower levels of secretion and/or intrinsic signaling capacity, or from a reduced ability to interact with putative intercellular transport machinery. To distinguish between these possibilities, we compared the mutant phenotypes with that of a hypomorphic *wg* allele, *Df(2)DE*, which produces a lower level of *wg* gene product in an otherwise normal expression pattern (Fig. 4A,B). Overall reduced Wg activity directs less naked cuticle specification, but all six of the wild-type denticle types (Bejsovec and Wieschaus, 1993) can be scored reproducibly (Figs 2, 4E,F, see inset). Thus, although the denticle-secreting cells lie at the greatest distance from the *wg*-expressing cells, the generation of denticle diversity requires only minimal amounts of Wg activity. In contrast, wg^{NE2} mutants (Fig. 4G, see inset) and wg^{NE1} mutants at 18°C secrete a less diverse array of denticles containing a disproportionate number of row-5-type denticles (Fig. 2), but show expanses of naked cuticle comparable to those of *Df(2)DE* embryos. Since a low level of wild-type Wg activity suffices to generate denticle diversity (Fig. 4F), the reduced diversity generated by the mutant molecules is unlikely to result solely from lower signaling activity. This raises the possibility that spatial constraints to mutant protein distribution are responsible for loss of cell fate diversity in the anterior portion of the segment.

Furthermore, *Df(2)DE* embryos produce considerable segmental patterning of dorsal cuticular elements (Fig. 4I,J), indicating that lowering overall Wg activity does not abolish dorsal signal transduction. In wg^{NE2} mutants, dorsal signaling is absent and the unpatterned dorsal surface is indistinguishable from that of a *wg* null mutant (Fig. 4K,L). This discrepancy between dorsal and ventral patterning is typical of all three partial function *wg* alleles, causing the mutant embryos to assume a curved shape. As discussed above, the dorsal-ventral distinction in patterning is also apparent in the Wg-mediated stabilization of *en* expression. In *Df(2)DE* embryos, *en* stabilization occurs in a continuous 1-cell-wide stripe (Cavallo et al., 1998), while the partial function mutants show stabilization in ventral cells only (Fig. 3J-L).

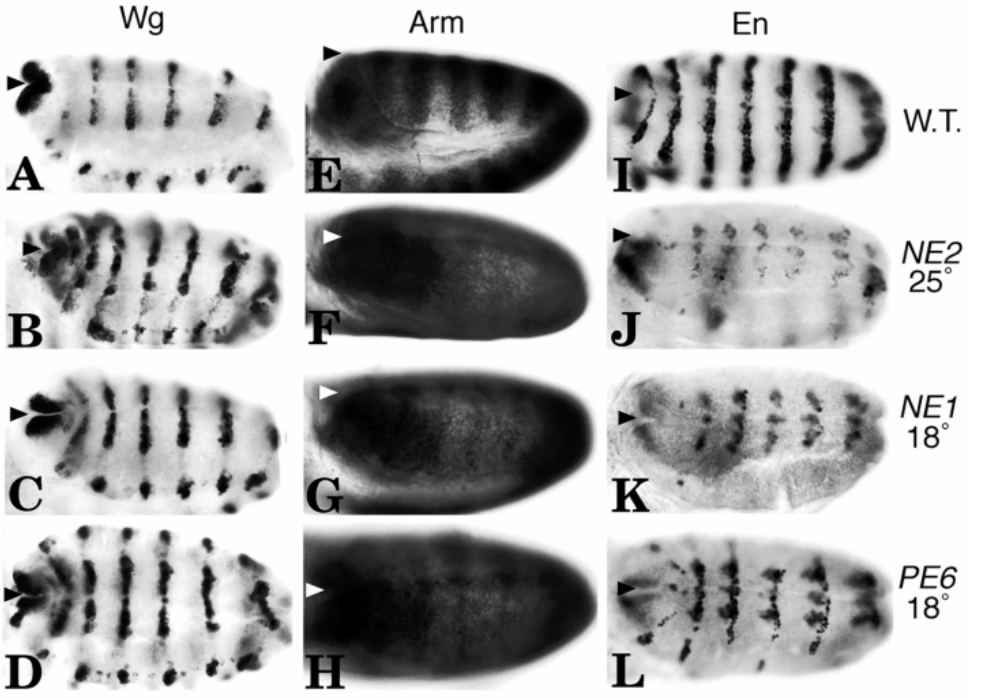

Fig. 3. Partial function mutants show restricted Wg protein distribution and reduced molecular response to Wg activity. (A) Wg antibody staining in abdominal segments of wild-type embryo. At earlier stages of development, the Wg stripe is continuous but by stage 11 (shown), lateral expression has ceased. Anterior of the embryo and posterior of extended germ band are to the left, arrowhead points to posterior end of ventral midline in all panels. Wg antibody staining in embryos mutant for (B) wg^{NE2}, (C) wg^{NE1} at 18°C and (D) wg^{PE6} at 18°C shows high accumulation of Wg protein. (E) Arm antibody staining shows broad stripes of high accumulation centered over the *wg*-expressing cells in stage 10 wild-type embryo. (F) wg^{NE2} mutant embryos at either 18 or 25°C show no Arm striping and resemble *wg* null mutants where only membrane-associated Arm is observed (Riggleman et al., 1990). At 18°C, (G) wg^{NE1} and (H) wg^{PE6} mutants show thin stripes of higher Arm. (I) *en* expression in epidermal cells posterior to the *wg*-expressing row is stabilized by wild-type Wg activity. (J) wg^{NE2} mutants show few *en*-expressing cells (Wg-independent *en* expression in the central nervous system is detected below the epidermal plane of focus). At 18°C, (K) wg^{NE1} and (L) wg^{PE6} mutants show more *en*-expressing ventral epidermal cells.

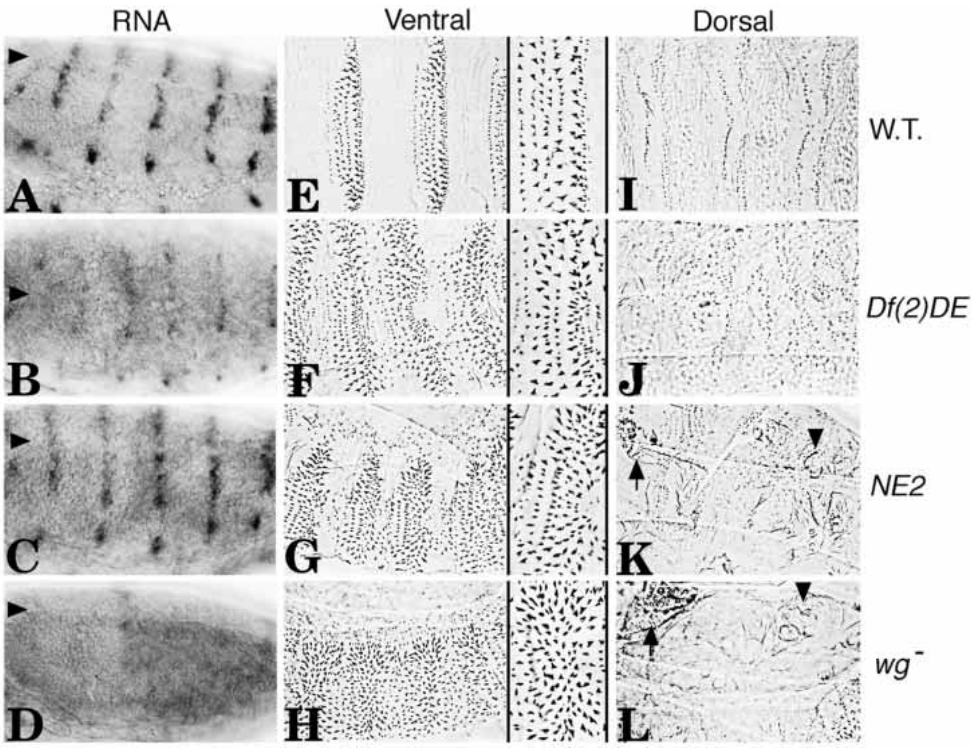

Fig. 4. Overall reduction of Wg function differs in phenotype from partial function alleles. (A) *wg* RNA in situ hybridization in stage 11 wild-type embryo compared with lower expression of *wg* RNA in (B) *Df(2)DE/wg^{CX4}* transheterozygous embryo at the same stage. *Df(2)DE/wg^{CX4}* mutant embryos show uniformly lower levels of *wg* expression throughout development. (C) *wg^{NE2}* mutants at stage 11 show near normal *wg* RNA levels. (D) In *wg^{IL114}* mutants at 25°C, *wg* expression decays prior to stage 11 (shown). (E) Wild-type embryos produce a ventral pattern with 6 rows of distinct denticle types separated by expanses of naked cuticle. Insets show anterior portion of fourth abdominal segment at higher magnification. (F) *Df(2)DE/wg^{CX4}* embryos display all 6 ventral denticle types, separated by small expanses of naked cuticle. (G) *wg^{NE2}* mutants show fewer ventral denticle types, but separated by comparable expanses of naked cuticle. (H) *wg^{CX4}* homozygotes secrete primarily a single denticle type. (I) Wild-type embryos display segmentally repeating dorsal cuticle structures. (J) *Df(2)DE/wg^{CX4}* mutants display segmentally repeating dorsal structures with slightly abnormal arrangement. (K) *wg^{NE2}* mutants show dorsal pattern defects identical to those of *wg^{CX4}* mutant embryos, (L) (Baker, 1988). Segmental pattern is abolished and dorsal expanse is greatly reduced: arrows indicate remnants of head cuticle and arrowheads indicate posterior terminal structures.

wg^{PE6}, *wg^{NE1}* and *wg^{NE2}* disrupt conserved residues

To detect the molecular lesions encoded by each partially functional *wg* allele, we performed RT-PCR with *wg*-specific primers on embryonic RNA. For each mutant stock, we sequenced the entire *wg* cDNA and verified putative mutational changes by restriction analysis. Each of the three lesions represents a single amino acid substitution within the coding sequence, presented schematically in Fig. 5A. *wg^{PE6}* encodes a missense mutation altering amino acid 136 from an alanine to valine (GCG to GTG). *wg^{NE1}* causes a glycine to aspartic acid change at residue 258 (GGC to GAC) and *wg^{NE2}* alters cysteine 242 to tyrosine (TGT to TAT).

All three residues affected are highly conserved throughout the Wnt family; alanine 136 and cysteine 242 are absolutely invariant in Wnts from *C. elegans* to humans, while glycine 258 is conserved among most members of the family (Fig. 5B). The *wg^{NE1}* and *wg^{NE2}* mutations are located near the truncation point, at residue 250, of the previously characterized, partially functional *wg^{PE4}* molecule (Bejsovec and Wieschaus, 1995).

Manipulated expression distinguishes between defective signaling versus transport

We expressed the mutant gene products under the control of the *GAL4-UAS* system (Brand and Perrimon, 1993). The *prd-GAL4* driver line allows us to compare short-range and long-range response to Wg signaling because it drives transgene expression in alternate segments (Yoffe et al., 1995) (Fig. 6A). When transgenes are driven in a *wg* null mutant, epidermal *en* expression is stabilized in cells within and immediately adjacent to the *prd* domain, but it is stabilized in the alternate segment only if the transgenic protein can accumulate in cells at a distance from the *prd* domain. For example, *prd-GAL4*-driven *UAS-wg^{+}* in a *wg* mutant background rescues *en* expression not only in the odd-numbered segments where it is expressed, but also in a ventral portion of the even-numbered segments (Hays et al., 1997). The ventral bias in rescue has led to speculation that Wg protein may be transported more efficiently through the ventral epidermis. Alternatively, only those cells may remain competent to respond by the time sufficient Wg has accumulated; earlier work with the temperature-sensitive *wg^{IL114}* allele has shown that this cell population is the last portion of the *en* stripe to be stabilized by Wg activity (Bejsovec and Martinez-Arias, 1991). Interestingly, at 18°C some rescue of *en* expression in dorsal cells is observed (Fig. 6F), suggesting that wild-type Wg protein may be slightly temperature sensitive for dorsal transport or signaling.

prd-GAL4-driven transgene expression rescues *en* expression in the ventral portion of the *prd* domain (Fig. 6F-J) and also expands it beyond the normal, 2-cell-wide, *en* domain, which is coincident with the posterior boundary of the *prd* domain (Yoffe et al., 1995). All three mutant transgenes show this expansion, suggesting that high-level expression promoted by the *GAL4-UAS* system increases paracrine signaling activity of the mutant molecules with respect to their activity under the endogenous *wg* promoter (Fig. 3I-L). Therefore the molecules may have slightly compromised signaling activity. However, their principal defect appears to be in transport. Even at these

high levels of expression, *prd-GAL4*-driven *UAS-wg^{NE1}* or *wg^{NE2}* at either temperature (Fig. 6G,H) does not stabilize *en* expression in the alternate segments, and only a few scattered ventral cells show stable *en* expression with *UAS-wg^{PE6}* at 25°C (Fig. 6I). Thus the mutant molecules are not able to move from odd-numbered segments, where they are expressed, to even-numbered segments. When constraints to transport are removed, by expressing the transgenes uniformly, ventral *en* expression is rescued in all segments (Fig. 6K-O), and excess naked cuticle is specified (not shown) as it is when wild-type Wg is ectopically expressed (Noordermeer et al., 1992; Hays et al., 1997). This indicates that the primary defect in the mutant molecules involves impaired movement through cells across the segment.

The *wg^{PE6}* mutant protein is highly temperature sensitive for this process. At 18°C, *prd-GAL4*-driven *UAS-wg^{PE6}* produces ventral rescue of *en* in alternate segments (Fig. 6J) equivalent to that observed with the wild-type transgene (Hays et al., 1997), indicating that transport of the mutant molecule is near normal at the lower temperature. Ectopic expression eliminates temperature-dependent ventral differences in *wg^{PE6}* function: uniform overexpression at 18°C and 25°C produce similar effects on ventral *en* expression (Fig. 6N,O) and on ventral cuticle pattern (not shown). However, dramatic differences are observed in dorsal regions, as discussed below.

Ventral and dorsal cell populations show differences in Wg response

Manipulated transgene expression reveals that dorsal epidermal cell populations respond differently to the mutant Wg molecules. These dorsoventral differences are not the result of differential expression, as each transgenic protein expressed with the *prd-GAL4* driver can be detected at equivalent levels in both ventral and dorsal portions of the *prd* domain (Fig. 6A,B). *prd-GAL4* driven *UAS-wg^{NE2}* (Fig. 6G) at either temperature and *UAS-wg^{NE1}* at 18°C (Fig. 6H) produce stabilization and slight expansion of *en* expression in ventral cells of the odd-numbered segments, while little or no stabilization is observed in dorsal regions of the *prd* domain. Since the *prd* domain partially overlaps the *en* expression domain (Yoffe et al., 1995), some of these dorsal cells are expressing transgenic protein. Therefore differential transport alone cannot account for the discrepancy; rather, some aspect of signal transduction in dorsal cells appears to be deficient. Furthermore, this effect is also observed when *E22C-GAL4* drives uniform overexpression of the mutant molecules: *en* expression is preferentially stabilized in ventral cells. In contrast, wild-type Wg expressed under the same conditions rescues and expands *en* expression with no difference in dorsal versus ventral regions (Fig. 6K).

UAS-wg^{PE6} produces slightly different patterns of *en* stabilization. At 25°C, *en* expression is rescued predominantly in the ventral portion of the *en* stripe, but this rescue extends into more dorsal regions than is observed with the other two mutant lines (Fig. 6I,N). At 18°C, *UAS-wg^{PE6}* stabilizes local *en* expression both ventrally and dorsally: in odd-numbered stripes when expressed with *prd-GAL4* (Fig. 6J), and in segmental stripes when driven ubiquitously (Fig. 6O). Furthermore, neither *UAS-wg^{PE6}* at 25°C (Fig. 6D), nor *UAS-wg^{NE1}* or *wg^{NE2}* at either temperature (Fig. 6C), rescue pattern

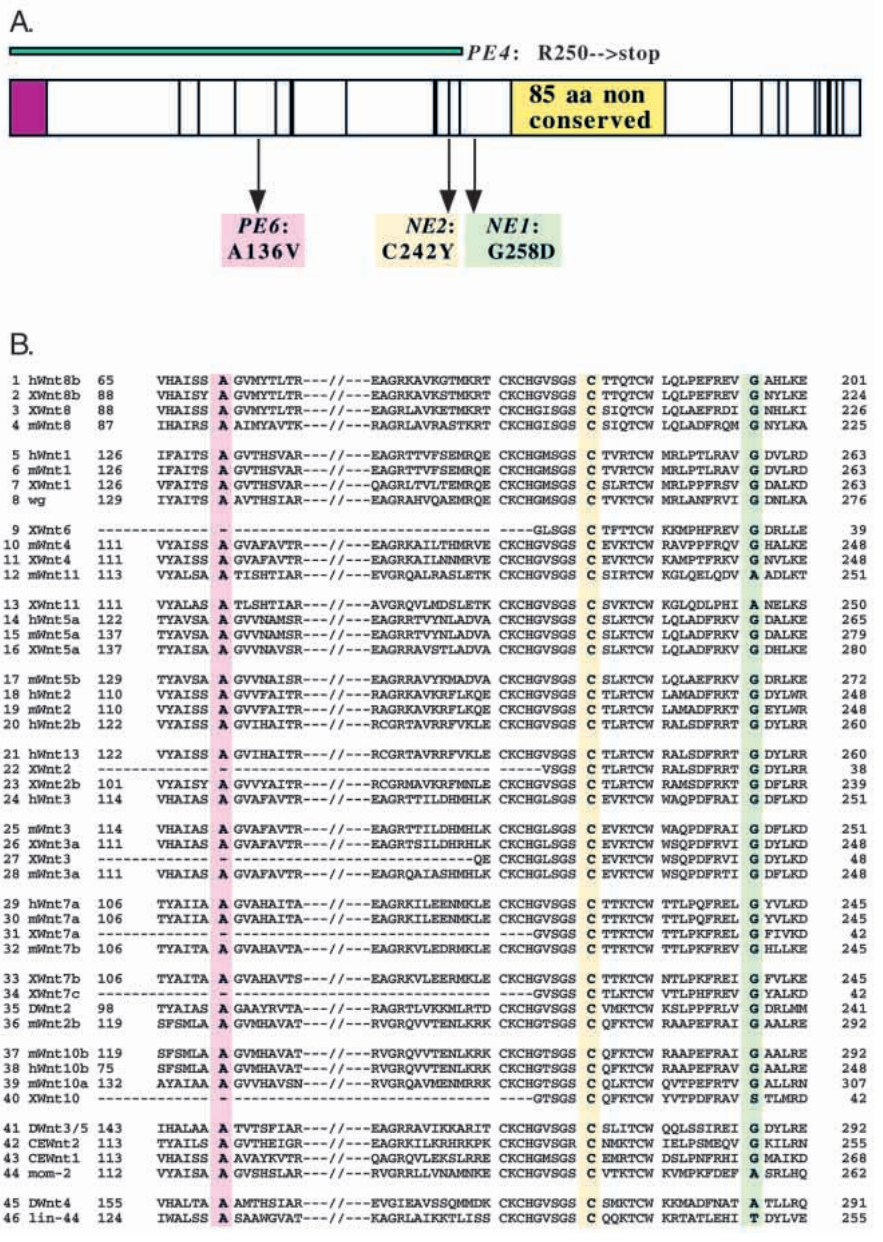

Fig. 5. Partial function *wg* mutations disrupt highly conserved residues. (A) Schematic diagram of Wg protein: purple box represents signal peptide, yellow box represents 85 amino acid nonconserved sequence, vertical lines represent cysteine residues conserved among all Wnt proteins. (B) *wg^{NE1}*, *wg^{NE2}* and *wg^{PE6}* amino acid substitutions (shaded residues) depicted with respect to the aligned sequences of known Wnt proteins, from *C. elegans* to humans.

elements in the dorsal cuticle when ectopically expressed with *E22C-GAL4*, but such expression of *UAS-wg^{PE6}* at 18°C shows substantial rescue of dorsal pattern (Fig. 6E). These observations indicate that both Wg-mediated dorsal signal transduction and Wg ligand transport are rendered temperature-sensitive by the *wg^{PE6}* mutant lesion.

Subcellular distribution of *wg^{PE6}* mutant protein is grossly abnormal even at 18°C

Confocal microscopy was used to compare the subcellular localization of the mutant Wg proteins with that of the wild-type Wg protein. Wg protein normally achieves a punctate distribution over several cell diameters on either side of the *wg*-expressing cells (van den Heuvel et al., 1989; Gonzalez et al., 1991). Vesicular staining can be detected in both apical and basal planes of focus within the epidermal cell layer (Fig. 7A,B). A comparable view of a *wg^{PE6}* homozygote at 25°C reveals that the mutant protein accumulates at high levels in the *wg*-expressing row of cells, with no punctate staining detectable in neighboring cells (Fig. 7C,D). This protein distribution is consistent with the severely restricted signaling activity observed in mutant embryos at 25°C. A superficially similar distribution is observed in *wg^{IL114}* mutant embryos at restrictive temperature and in *porcupine* mutant embryos, which appear to be defective in export of Wg protein (van den Heuvel et al., 1994). However, in these situations, no Wg signaling activity can be detected, whereas *wg^{PE6}* homozygotes at 25°C clearly retain some Wg function, as measured by cuticle pattern and autocrine effects on *wg* expression.

In *wg^{PE6}* homozygotes at 18°C, Wg protein can be detected over a broader domain of cells, encompassing the *wg*-expressing row and its immediate neighbors (Fig. 7E,F). In contrast to the vesicular appearance of wild-type Wg, the *wg^{PE6}* mutant protein appears to accumulate preferentially around the cell membranes. This is particularly obvious in the more basal plane of focus (Fig. 7F), where high levels of Wg staining surround the basolateral cell membranes in both *wg*-expressing and non-*wg*-expressing cells. However, punctate staining is also detected within these cells, suggesting that some protein can be internalized properly in vesicles.

DISCUSSION

We have identified and characterized three new mutations in the Wg molecule that retain some signaling activity but show

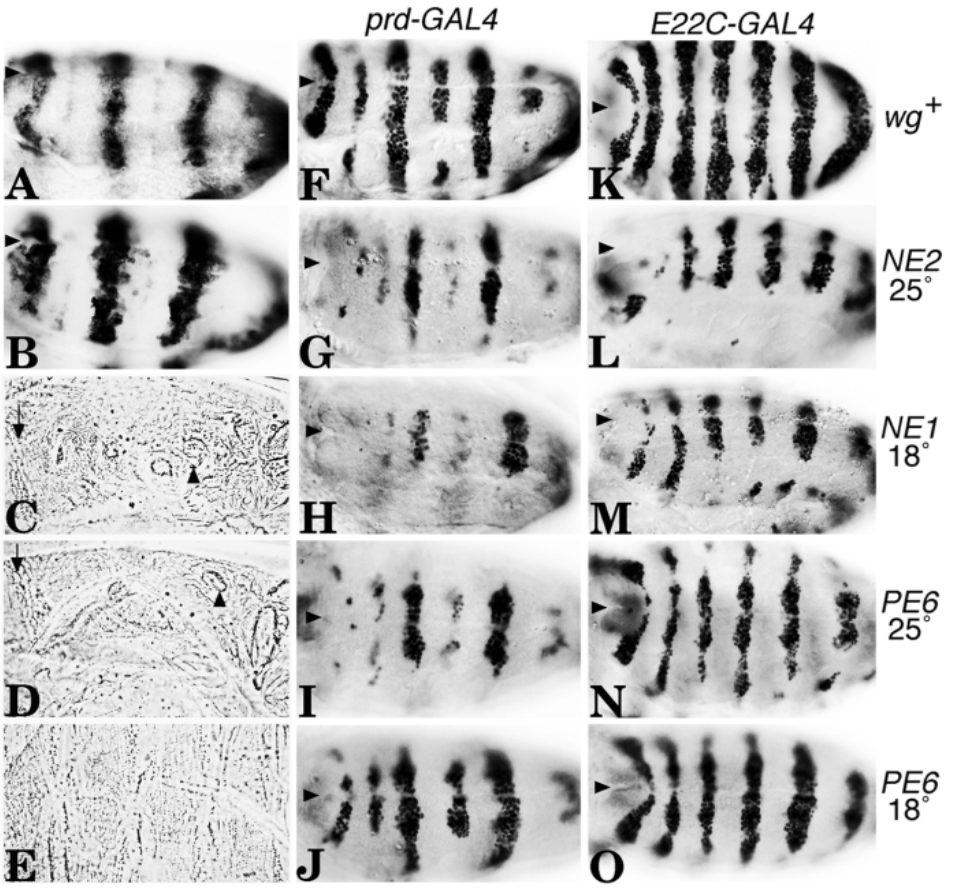

Fig. 6. Ventral transport and dorsal signaling are disrupted by partial function mutations. Wg antibody staining in wild-type stage 11 embryo with *prd-GAL4*-driven (A) *UAS-wg^{+}* and (B) *UAS-wg^{NE2}* expression. Transgene expression in odd-numbered segments is much higher than endogenous *wg* expression in even-numbered segments. Arrowhead (A,B,F-O) indicates posterior end of extended germ band. Dorsal cuticle pattern of a *wg^{CX4}* mutant is not rescued by *E22C-GAL4*-driven overexpression of (C) *UAS-wg^{NE1}* at 18°C or (D) *UAS-wg^{PE6}* at 25°C. Embryos assume a curved shape because dorsal expanse is greatly reduced: arrows indicate hairs typical of anterior region and arrowheads indicate posterior terminal structures. Substantial rescue of dorsal pattern elements are observed with *E22C-GAL4*-driven overexpression of (E) *UAS-wg^{PE6}* at 18°C. Embryos show normal segmentation and are of wild-type length and shape. Compare with wild-type and *wg* mutant dorsal patterns in Fig. 4I,L. En antibody staining of *wg^{CX4}* mutant with *prd-GAL4*-driven (F) *UAS-wg^{+}* at 18°C shows rescue of *en* expression locally in odd-numbered segments and long-range in even-numbered segments, (G) *UAS-wg^{NE2}* and (H) *UAS-wg^{NE1}* at 18°C rescue *en* expression only in the ventral portion of odd-numbered segments, (I) *UAS-wg^{PE6}* at 25°C rescues *en* expression predominantly in the ventral portion of odd-numbered segments and slightly in even-numbered segments. (J) *UAS-wg^{PE6}* at 18°C rescues *en* stripe entirely in odd-numbered segments and in ventral portion of even-numbered segments. This pattern is identical to that observed for *prd-GAL4*-driven *UAS-wg^{+}* at 25°C (Hays et al., 1997). *wg^{CX4}* mutant with uniform *E22C-GAL4*-driven expression of (K) *UAS-wg^{+}* at 25°C rescues entire *en* stripe, with strong expression in both dorsal and ventral regions. *E22C-GAL4*-driven expression of (L) *UAS-wg^{NE2}* and (M) *UAS-wg^{NE1}* at 18°C rescue *en* primarily in ventral regions, (N) *UAS-wg^{PE6}* at 25°C rescues *en* more substantially, with strong expression in the ventralmost domain, (O) *UAS-wg^{PE6}* at 18°C rescues entire *en* stripe, with strong expression in both dorsal and ventral regions.

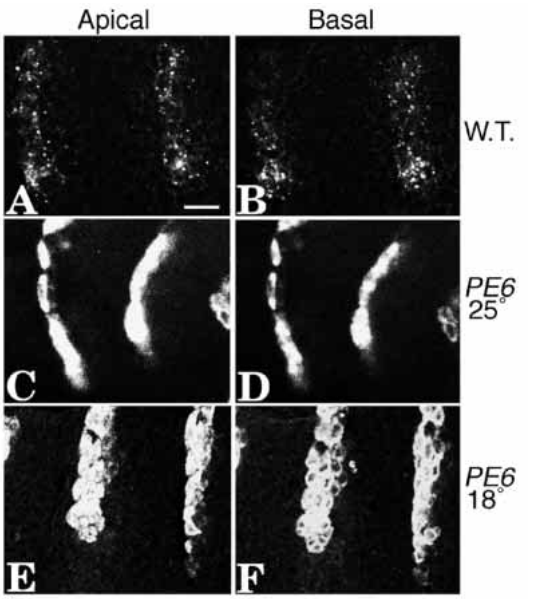

Fig. 7. wg^{PE6} protein shows abnormal subcellular localization even at 18°C. (A) Confocal micrograph of Wg antibody staining in the fifth and sixth abdominal segment of a wild-type stage 11 embryo. Ventral midline is at top, posterior of germ band to the left. Scale bar is 10 μm. (B) More basal plane of focus within the epidermal layer shows similar vesicular staining. (C,D) wg^{PE6} protein at 25°C accumulates at high levels in *wg*-expressing row of cells, with no vesicles apparent in neighboring epidermal cells at any plane of focus. Similar Wg protein distributions are observed in wg^{NE1} and wg^{NE2} mutant embryos. (E,F) wg^{PE6} protein at 18°C is detected in additional rows of cells, but shows aberrant localization around the cell periphery, particularly in basolateral regions (F).

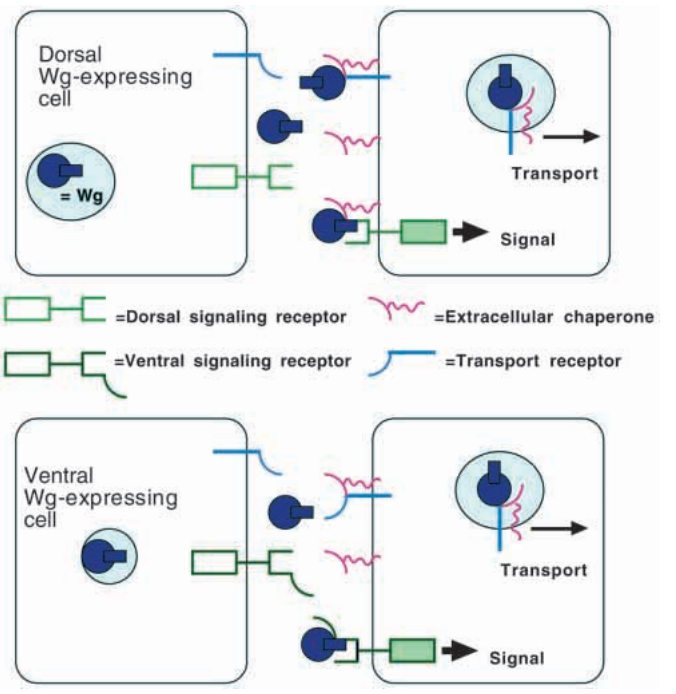

Fig. 8. Model for wild-type Wg signaling in dorsal versus ventral cell populations. Partial function *wg* mutations disrupt binding to a putative extracellular chaperone, which is required for intercellular Wg protein transport and for dorsal cell-specific paracrine signaling, but is dispensable for autocrine activity and ventral cell-specific paracrine signaling.

dramatic defects due to impaired protein distribution across the epidermal cells of the embryonic segment. Two of the three mutations, wg^{NE1} and wg^{NE2}, are located near the truncation point of a previously described transport defective molecule, wg^{PE4} (Hays et al., 1997). This suggests that a region near the midpoint of the Wg protein sequence may be involved in intercellular ligand transport. The third mutation, wg^{PE6}, alters a residue in a more aminoterminal position and shows a highly temperature-sensitive defect in transport. These molecules are able to stabilize *en* expression in neighboring ventral cell populations. This local paracrine response indicates that they are exported to the cell surface properly. We propose that the defect in each blocks interaction of the ligand with cell surface or extracellular molecules that promote movement around, or entry into, neighboring rows of cells. The aberrant subcellular localization of wg^{PE6} protein, even at 18°C where transport is largely restored, suggests that the mutant lesion alters contacts between Wg and other cellular components.

Recent work has implicated the putative Wg receptor, Dfrizzled2 (Dfz2), as a potential candidate for a cell surface molecule involved somehow in Wg transport (Cadigan et al., 1998). Overexpression of Dfz2 in the wing imaginal disc produces a broader distribution of the endogenous Wg protein, enhancing its activity in cells at a distance from the *wg*-expressing domain of cells. This contrasts with other growth factor receptors, which sequester ligand when overexpressed (Stein et al., 1991; Chen and Struhl, 1996). Although Dfz2 can act as an extracellular chaperone for Wg in the context of the wing disc, it does not appear to play an analogous role in the embryonic epidermis. Embryos overexpressing Dfz2 hatch into viable larvae with cuticle patterns that do not display Wg hyperactivity (A.B., unpublished). Another class of potential extracellular chaperone are proteoglycans: glycosaminoglycans appear to be essential for Wg signal transduction (Reichsman and Cumberledge, 1996). The extracellular sugar groups are thought to increase the local concentration of Wg ligand and thereby improve signaling efficiency. Overexpressing Wg can bypass the requirement and rescue pattern defects caused by mutations in glycosaminoglycan biosynthesis (Binari et al., 1997; Häcker et al., 1997).

In ventral epidermal cells, the wg^{NE1}, wg^{NE2} and wg^{PE6} mutant molecules show substantial signaling activity when ectopically expressed. This supports the idea that their primary defect is impaired transport. In dorsal cell populations, however, none of the three mutant molecules are able to trigger normal molecular and morphological responses to Wg even at high levels of expression. Thus there appears to be a link between Wg protein transport and dorsal Wg signal transduction: each of three amino acid substitutions alters both aspects of Wg function simultaneously. It is formally possible that these defects represent altered ligand interaction with two independent sets of molecules. However, for reasons of parsimony, we propose that each mutation decreases binding affinity for a single extracellular chaperone, which is exclusive to the transport machinery in ventral epidermal cells but is shared with signal transduction machinery in dorsal cells (Fig. 8). A corollary of this model is that the ventral and dorsal signaling receptors must be distinct,

since ventrally the proposed chaperone is not essential for signal transduction. Furthermore, the autocrine function of Wg in maintaining its own expression may not require this chaperone, as dorsal *wg* autoregulation is not disrupted by the mutant lesions.

This model would also explain a previously observed temporal link between Wg specification of dorsal pattern elements and ventral denticle diversity. Temperature-shift experiments with the wg^{IL114} allele (Bejsovec and Martinez-Arias, 1991) showed that denticle diversity and all dorsal pattern are generated by Wg signaling activity during stages 9 and 10, while Wg activity during stages 11 and 12 directs cells to secrete naked cuticle. Embryos that are shifted down to permissive temperature at stage 11 show small expanses of naked cuticle in a lawn of uniform denticles, with no detectable rescue of dorsal pattern elements; this pattern is very similar to that of the partially functional *wg* mutants described here. These observations could be explained if the proposed extracellular chaperone is present only at early stages of development. Late stage restoration of Wg function then would be unable to rescue either aspect of the pattern: ventrally, the restored Wg protein would not be transported properly to perform long-range diversity generation, and dorsally it would not signal efficiently. During wild-type embryonic patterning, such temporal changes in a chaperone might contribute to the restriction of Wg activity in later stages of development. This would favor accumulation of high-level Wg to promote naked cuticle cell fate close to the *wg*-expressing row and would protect denticle cell fates from respecification to naked cuticle by inappropriate Wg activity.

We wish to thank M. Peifer, E. Wieschaus and S. Cumberledge for antibodies, R. Nusse and J. Pradel for fly stocks, and members of the Bejsovec, Holmgren and Andres laboratories for discussions. We are also grateful to M. Moline for technical assistance. This work was supported in part by a Gramm Travel Fellowship Award to H. A. D. from the Lurie Cancer Center of Northwestern University and by a CAREER Award to A. B. from the National Science Foundation, Grant No. IBN-9734072.

REFERENCES

Baker, N. E. (1987). Molecular cloning of sequences from *wingless*, a segment polarity gene in *Drosophila*: the spatial distribution of a transcript in embryos. *EMBO J.* **6**, 1765-1773.

Baker, N. E. (1988). Embryonic and imaginal requirements for *wingless*, a segment polarity gene in *Drosophila*. *Dev. Biol.* **125**, 96-108.

Bejsovec, A. and Martinez-Arias, A. (1991). Roles of *wingless* in patterning the larval epidermis of *Drosophila*. *Development* **113**, 471-485.

Bejsovec, A. and Peifer, M. (1996). The *wingless/Wnt-1* signaling pathway – new insights into the cellular mechanisms of signal transduction. *Advances in Developmental Biochemistry* **4**, 1-45.

Bejsovec, A. and Wieschaus, E. (1993). Segment polarity gene interactions modulate epidermal patterning in *Drosophila* embryos. *Development* **119**, 501-517.

Bejsovec, A. and Wieschaus, E. (1995). Signaling activities of the *Drosophila wingless* gene are separately mutable and appear to be transduced at the cell surface. *Genetics* **139**, 309-320.

Binari, R. C., Staveley, B. E., Johnson, W. A., Godavarti, R., Sasisekharan, R. and Manoukian, A. S. (1997). Genetic evidence that heparin-like glycosaminoglycans are involved in wingless signaling. *Development* **124**, 2623-2632.

Bradley, R. S. and Brown, A. M. C. (1990). The proto-oncogene *int* -1 encodes a secreted protein associated with the extracellular matrix. *EMBO J.* **9**, 1569-1575.

Brand, A. H. and Perrimon, N. (1993). Targeted gene expression as a means of altering cell fates and generating dominant phenotypes. *Development* **118**, 401-415.

Brunner, E., Peter, O., Schweizer, L. and Basler, K. (1997). *pangolin* encodes a Lef-1 homolog that acts downstream of Armadillo to transduce the Wingless signal. *Nature* **385**, 829-833.

Buenzow, D. and Holmgren, R. (1995). Expression of the *Drosophila gooseberry* locus defines a subset of neuroblast lineages in the central nervous system. *Dev. Biol.* **170**, 338-349.

Cadigan, K. M., Fish, M. P., Rulifson, E. J. and Nusse, R. (1998). Wingless repression of *Drosophila frizzled 2* expression shapes the Wingless morphogen gradient in the wing. *Cell* **93**, 767-777.

Campos-Ortega, J. A. and Hartenstein, V. (1985). *The Embryonic Development of Drosophila melanogaster.* Berlin: Springer-Verlag.

Cavallo, R. A., Cox, R. T., Moline, M. M., Roose, J., Polevoy, G. A., Clevers, H., Peifer, M. and Bejsovec, A. (1998). *Drosophila* TCF and Groucho interact to repress Wingless signaling activity. *Nature* **395**, 604-608.

Chen, Y. and Struhl, G. (1996). Dual roles for patched in sequestering and transducing hedgehog. *Cell* **87**, 553-563.

Dierick, H. and Bejsovec, A. (1998). Cellular mechanisms of Wingless/Wnt signaling activity. In *Current Topics in Developmental Biology* (ed. Pederson and G. Schatten). New York: Academic Press. (In press).

DiNardo, S., Sher, E., Heemskerk-Jongens, J., Kassis, J. A. and O'Farrell, P. (1988). Two-tiered regulation of spatially patterned *engrailed* gene expression during *Drosophila* embryogenesis. *Nature* **322**, 604-609.

Dougan, S. and DiNardo, S. (1992). *Drosophila wingless* generates cell type diversity among *engrailed* expressing cells. *Nature* **360**, 347-350.

Gonzalez, F., Swales, L., Bejsovec, A., Skaer, H. and Martinez Arias, A. (1991). Secretion and movement of the *wingless* protein in the *Drosophila* embryo. *Mech. Dev.* **35**, 43-54.

Häcker, U., Lin, X. and Perrimon, N. (1997). The Drosophila *sugarless* gene modulates Wingless signaling and encodes an enzyme involved in polysaccharide biosynthesis. *Development* **124**, 3565-3573.

Hays, R., Gibori, G. B. and Bejsovec, A. (1997). Wingless signaling generates epidermal pattern through two distinct mechanisms. *Development* **124**, 3727-3736.

Ingham, P. W. and Hidalgo, A. (1993). Regulation of *wingless* transcription in the *Drosophila* embryo. *Development* **117**, 283-291.

Jue, S. F., Bradley, R. S., Rudnicki, J. A., Varmus, H. E. and Brown, A. M. C. (1992). The mouse *Wnt-1* gene can act via a paracrine mechanism in transformation of mammary epithelial cells. *Mol. Cell. Biol.* **12**, 321-328.

Lohs-Schardin, M., Cremer, C. and Nüsslein-Volhard, C. (1979). A fate map for the larval epidermis of *Drosophila melanogaster*: localized cuticle defects following irradiation of the blastoderm with a UV laser microbeam. *Dev. Biol.* **73**, 239-255.

Martinez Arias, A., Baker, N. and Ingham, P. (1988). Role of the segment polarity genes in the definition and maintenance of cell states in the *Drosophila* embryo. *Development* **103**, 157-170.

Mostov, K. E. (1994). Transepithelial transport of immunoglobulins. *Annual Review of Immunology* **12**, 63-84.

Noordermeer, J., Johnston, P., Rijsewijk, F., Nusse, R. and Lawrence, P. A. (1992). The consequences of ubiquitous expression of the *wingless* gene in the *Drosophila* embryo. *Development* **116**, 711-719.

Nusse, R., Samos, C. H., Brink, M., Willert, K., Cadigan, K. M., Fish, M. and Rulifson, E. (1997). Cell culture and whole animal approaches to understanding signaling by Wnt proteins in *Drosophila*. *Cold Spring Harbor Symp. Quant. Biol.* **62**, 185-190.

Nusse, R. and Varmus, H. E. (1992). *Wnt* genes. *Cell* **69**, 1073-1087.

Nüsslein-Volhard, C. and Wieschaus, E. (1980). Mutations affecting segment number and polarity in *Drosophila*. *Nature* **287**, 795-801.

Papkoff, J. and Schryver, B. (1990). Secreted *int-1* protein is associated with the cell surface. *Mol. Cell. Biol.* **10**, 2723-2730.

Parkin, N. T., Kitajewski, J. and Varmus, H. E. (1993). Activity of Wnt-1 as a transmembrane protein. *Genes Dev.* **7**, 2181-2193.

Peifer, M., Rauskolb, C., Williams, M., Riggleman, B. and Wieschaus, E. (1991). The segment polarity gene *armadillo* affects the *wingless* signalling pathway in both embryonic and adult pattern formation. *Development* **111**, 1028-1043.

Reichsman, F. and Cumberledge, S. (1996). Glycosaminoglycans can modulate extracellular localization of the wingless protein and promote signal transduction. *J. Cell Biol.* **135**, 819-827.

Riese, J., Yu, X., Munnerlyn, A., Eresh, S., Hsu, S.-C., Grosschedl, R. and Bienz, M. (1997). LEF-1, a nuclear factor coordinating signalling inputs from *wingless* and *decapentaplegic*. *Cell* **88**, 777-787.

Riggleman, B., Schedl, P. and Wieschaus, E. (1990). Spatial expression of the *Drosophila* segment polarity gene *armadillo* is post-transcriptionally regulated by *wingless*. *Cell* **63**, 549-560.

Rijsewijk, F., Schuermann, M., Wagenaar, E., Parren, P., Weigel, D. and Nusse, R. (1987). The *Drosophila* homologue of the mouse mammary oncogene *int-1* is identical to the segment polarity gene *wingless*. *Cell* **50**, 647-657.

Rodman, J. S., Mercer, R. W. and Stahl, P. D. (1990). Endocytosis and transcytosis. *Current Opinion in Cell Biology* **2**, 664-72.

Sampedro, J., Johnston, P. and Lawrence, P. A. (1993). A role for *wingless* in the segmental gradient of *Drosophila*? *Development* **117**, 677-687.

Sharma, R. P. and Chopra, V. L. (1976). Effects of the *wingless (wg^1)* mutation on wing and haltere development in *Drosophila melanogaster*. *Dev. Biol.* **48**, 461-465.

Spradling, A. C. (1986). P-element mediated transformation. In *Drosophila: A Practical Approach* (ed. D. B. Roberts), pp. 175-198. Oxford: IRL Press.

Stein, D., Roth, S., Vogelsang, E. and Nüsslein-Volhard, C. (1991). The polarity of the dorsoventral axis in the *Drosophila* embryo is defined by an extracellular signal. *Cell* **65**, 725-735.

Tautz, D. and Pfeifle, C. (1989). A non-radioactive in situ hybridization method for the localization of specific RNAs in *Drosophila* embryos reveals translational control of the segmentation gene *hunchback*. *Chromosoma* **98**, 81-85.

Tiong, S. Y. K. and Nash, D. (1990). Genetic analysis of the *adenosine3 (Gart)* region of the second chromosome in *Drosophila melanogaster*. *Genetics* **124**, 889-897.

van de Wetering, M., Cavallo, R., Dooijes, D., van Beest, M., van Es, J., Loureiro, J., Ypma, A., Hursh, D., Jones, T., Bejsovec, A. et al. (1997). Armadillo co-activates transcription driven by the product of the *Drosophila* segment polarity gene *dTCF*. *Cell* **88**, 789-799.

van den Heuvel, M., Harryman-Samos, C., Klingensmith, J., Perrimon, N. and Nusse, R. (1994). Mutations in the segment polarity genes *wingless* and *porcupine* impair secretion of the wingless protein. *EMBO J.* **12**, 5293-5302.

van den Heuvel, M., Nusse, R., Johnston, P. and Lawrence, P. A. (1989). Distribution of the *wingless* gene product in *Drosophila* embryos: a protein involved in cell-cell communication. *Cell* **59**, 739-749.

van der Bliek, A. M. and Meyerowitz, E. M. (1991). Dynamin-like protein encoded by the *Drosophila shibire* gene associated with vesicular traffic. *Nature* **351**, 411-414.

Wieschaus, E. and Nüsslein-Volhard, C. (1986). Looking at embryos. In *Drosophila, A Practical Approach* (ed. D. B. Roberts). Oxford, UK: IRL Press.

Yoffe, K. B., Manoukian, A. S., Wilder, E. L., Brand, A. S. and Perrimon, N. (1995). Evidence for *engrailed*-independent *wingless* autoregulation in *Drosophila*. *Dev. Biol.* **170**, 636-650.

Zecca, M., Basler, K. and Struhl, G. (1996). Direct and long-range action of a *wingless* morphogen gradient. *Cell* **87**, 833-844.